Molecular Biology of the Cell
Vol. 21, 1335–1349, April 15, 2010

Deficiency of the Transcriptional Regulator p8 Results in Increased Autophagy and Apoptosis, and Causes Impaired Heart Function

Derek K. Kong,* Serban P. Georgescu,* Carla Cano,† Mark J. Aronovitz,* Juan Lucio Iovanna,† Richard D. Patten,* John M. Kyriakis,* and Sandro Goruppi*

*Molecular Cardiology Research Institute, Tufts Medical Center and Department of Medicine, Tufts University School of Medicine, Boston, MA 02111; and †Institut National de la Santé et de la Recherche Médicale, Unite' 624 "Stress Cellulaire," 13288 Marseille Cedex 9, France

Submitted September 23, 2009; Revised December 24, 2009; Accepted February 16, 2010
Monitoring Editor: Jonathan Chernoff

Autophagy is a cytoprotective pathway used to degrade and recycle cytoplasmic content. Dysfunctional autophagy has been linked to both cancer and cardiomyopathies. Here, we show a role for the transcriptional regulator p8 in autophagy. *p8* RNA interference (RNAi) increases basal autophagy markers in primary cardiomyocytes, in H9C2 and U2OS cells, and decreases cellular viability after autophagy induction. This autophagy is associated with caspase activation and is blocked by *atg5* silencing and by pharmacological inhibitors. FoxO3 transcription factor was reported to activate autophagy by enhancing the expression of autophagy-related genes. P8 expression represses FoxO3 transcriptional activity, and *p8* knockdown affects FoxO3 nuclear localization. Thus, *p8* RNAi increases FoxO3 association with *bnip3* promoter, a known proautophagic FoxO3 target, resulting in higher *bnip3* RNA and protein levels. Accordingly, *bnip3* knockdown restores cell viability and blocks apoptosis of *p8*-deficient cells. In vivo, *p8* −/− mice have higher autophagy and express higher cardiac *bnip3* levels. These mice develop left ventricular wall thinning and chamber dilation, with consequent impaired cardiac function. Our studies provide evidence of a p8-dependent mechanism regulating autophagy by acting as FoxO3 corepressor, which may be relevant for diseases associated with dysregulated autophagy, as cardiovascular pathologies and cancer.

INTRODUCTION

Autophagy is a cellular response to insufficient nutrient availability and stress, which involves the sequestration of cytosol and organelles within autophagosomes for their delivery to lysosomes (Xie and Klionsky, 2007; Klionsky *et al*., 2008). Through autophagy, cells recycle and generate new metabolic substrates and adapt to reduced nutrient availability (Kundu and Thompson, 2008; Meijer and Codogno, 2008). Autophagy eliminates toxic proteins, damaged and aged cells or organelles, and can eventually elicit a self-destructive system leading to cell death (Baehrecke, 2005; Maiuri *et al*., 2007). Accordingly, the disruption of this process is associated with multiple pathophysiological conditions, including cancer, diabetes, and cardiovascular diseases (Levine and Kroemer, 2008; Mizushima *et al*., 2008).

In unstressed cells, autophagy is inhibited by the mammalian target of rapamycin complex 1 (mTORC1). Nutrient depletion, serum starvation, rapamycin inhibition of mTORC1, or activation of 5′AMP-activated protein kinase (AMPK) by 5-aminoimidazole-4-carboxamide-1-D-ribofuranoside (AICAR) promotes the activation of a set of autophagy-regulating proteins (Atg). In turn, some Atgs contribute to the formation of the autophagosomes, which contain the cellular components destined for degradation (Klionsky *et al*., 2008; Kundu and Thompson, 2008).

Autophagy requires two ubiquitin-like systems, one leading to the conjugation of Atg12 to Atg5 and the second converting the microtubule-associated protein 1 light chain 3 (LC3 or Atg8) soluble form (LC3-I) to the autophagic vesicle-associated form (LC3-II) (Klionsky *et al*., 2008).

Aside from cellular relocalization and posttranslational modifications of Atgs, the autophagic process includes the activation of a transcriptional program (Attaix and Bechet, 2007). Up-regulation of lysosomal enzymes, such as cathepsin L, and of multiple *atg* genes has been reported in several cell systems and organisms (Attaix and Bechet, 2007; Meijer and Codogno, 2008). Indeed, the transcription factor E2F was shown to drive *lc3*, *atg1*, and *dram* expression in U2OS cells, whereas the transcription factor FoxO3 was shown to control the expression of *bnip3*, *beclin1*, and *lc3* among others, in cultured myocytes and in vivo (Mammucari *et al*., 2007; Zhao *et al*., 2007; Polager *et al*., 2008). However, the mechanisms involved in the fine-tuning, repression, and termination of this cellular program are still poorly investigated.

In the heart, autophagy is important for the turnover of organelles at low basal levels under normal conditions (Nakai *et al*., 2007). Cardiac basal autophagy is altered by stress triggered by cardiovascular diseases, including ischemic in-

This article was published online ahead of print in *MBoC in Press* (http://www.molbiolcell.org/cgi/doi/10.1091/mbc.E09–09–0818) on February 24, 2010.

Address correspondence to: Sandro Goruppi (sgoruppi@tuftsmedicalcenter.org) or John M. Kyriakis (jkyriakis@tuftsmedicalcenter.org).

jury, cardiac hypertrophy, cardiac remodeling, and heart failure (De Meyer and Martinet, 2008; Rothermel and Hill, 2008a). Basal autophagy seems to play a protective role, because *atg7* silencing in rat neonatal cardiomyocytes reduces cell viability, and adult cardiomyocytes from cardiac-specific *atg5*-deficient hearts are more susceptible to isoproterenol (Nakai *et al*., 2007). Yet, its role in the heart is still poorly understood.

p8 (nupr1 or com1) is a nuclear basic helix-loop-helix protein strongly induced in response to stress (Chowdhury *et al*., 2009; Goruppi and Iovanna, 2009). p8 has been implicated in several diverse context-dependent functions, including transcriptional regulation, cell cycle control, diabetic renal and cardiomyocyte hypertrophy, as well as apoptotic regulation (Goruppi *et al*., 2002, 2007; Vasseur *et al*., 2002b; Quirk *et al*., 2003; Carracedo *et al*., 2006; Malicet *et al*., 2006; Salazar *et al*., 2009; Sambasivan *et al*., 2009). Accordingly, p8 acts as a transcriptional coactivator and interacts with members of the transcriptional machinery, including AP1 complex, p53, and p300, among others (Hoffmeister *et al*., 2002; Goruppi *et al*., 2007; Clark *et al*., 2008).

We have shown that p8 is induced in failing human hearts. p8 is a transcriptional regulator required for endothelin-1– and phenylephrine-induced hypertrophy in rat cardiomyocytes and for tumor necrosis factor (TNF)-induced activation of matrix metalloprotease (MMP) 9 in rat cardiac fibroblasts (Goruppi *et al*., 2007). Accordingly, p8 associates with and activates the *MMP9* promoter in primary fibroblasts and cancer cells.

In this study, we investigate a role for p8 in autophagy in vitro and in vivo, by using the *p8* $-/-$ mice. In both settings, silencing of *p8* is associated with basal up-regulation of autophagy and apoptosis. In vivo, the hearts of *p8* knockout mice develop features that provoke a decreased left ventricular functionality.

MATERIALS AND METHODS

Cell Culture and Treatments

U2OS, 293, and H9C2 cells were cultured in DMEM supplemented with 10% fetal bovine serum (FBS). Primary rat cardiomyocytes, human cardiac fibroblasts, and human aortic endothelial cells were from ScienCell Research Laboratories (Carlsbad, CA). Rapamycin, AICAR, 2-deoxyglucose (2DG), 3-methyladenine, methyl pyruvate, TNF, zVADfmk, E64D, pepstatin, puromycin, and G418 were all from Calbiochem (San Diego, CA). Survival assays and 3-(4,5-dimethylthiazol-2-yl)-2,5-diphenyltetrazolium bromide (MTT; Calbiochem) labeling of the cells were performed as reported previously (Goruppi *et al*., 2001). In brief, the U2OS cells were seeded in 12-well tissue culture dishes and were transfected the following day, when 60–70% confluent, with either *crtl* or *p8* small interfering RNA (siRNA) by using the Transit Plus transfection reagent (Mirus, Madison, WI), as indicated by the manufacturer. After 48 h, the cells were treated as indicated for further 48 h; the culture medium was then changed with fresh medium containing 10% FBS and 10 mg/ml MTT, and the cultures labeled for 4 h. All experiments were carried out in triplicate. Formazan salt products were solubilized in 10% SDS and 0.1 M HCl for the spectrophotometric quantification.

Reverse Transcription-Polymerase Chain Reaction (RT-PCR)

Total RNA was isolated and RT-PCRs were performed as described in Goruppi *et al*. (2002). *β-actin* or *gapdh* served as controls. Primer sequences were as follows: for human *p8*, ATGGCCACCTTCCCACCAGCAA sense and GGCTGCCGTGCGTGTCTATTTA antisense; for mouse *lc3*, CGTCCTGGACAAGACCAAGT sense and ATGTGGGTGCCTACGTTCTC antisense; and for mouse *bnip3*, GGGTTTTCCCCAAAGGAATA sense and GACCACCCAAGGTAATGGTG antisense.

siRNA Interference, Cellular Fractionation, and Chromatin Immunoprecipitation (ChIP)

For human *p8* siRNA, we used two pairs of oligonucleotides (OLs), which silenced both at a similar extent the endogenous *p8*. Rat p8 siRNA has been described in Goruppi *et al*. (2002). sc-37007, sc-41445, sc-37451 (Santa Cruz Biotechnology, Santa Cruz, CA) were used for control (*ctrl*), *atg5*, and *bnip3* RNAi, respectively. In some experiments, control oligonucleotides were a mix of two nontargeting sequences. For ChIPs, 24 h after *p8* or *crtl* RNAi U2OS cells were kept in 10% FBS or serum starved for 20 h, as indicated. ChIPs were performed using SimpleChIP Enzymatic Chromatin IP kit (Cell Signaling Technology, Danvers, MA). Human *p8*, OL1: GGAGGACCCAGGACAGGATTT sense and AAATCCTGTCCTGGGTCCTCC antisense, and OL2 were from Carracedo *et al*. (2006). Annealed siRNAs were introduced in the cells using Transit Plus transfection reagent (Mirus), as indicated by the manufacturer. In each experiment, the effective gene silencing was monitored by RT-PCR. *p8* and control lentiviruses, which contain three to five target-specific hairpin constructs to knockdown gene expression (or a nontargeting mix control), were from Santa Cruz Biotechnology. U2OS cells were infected as indicated by the manufacturer and selected for one week with 3 μg/ml puromycin.

Nuclear/Cytosol (N/C) Separation. U2OS cells either overexpressing or having *p8* silenced or infected with *crtl* virus were grown to confluence in 10-cm cell culture dishes and then either serum starved for 24 h or left in complete culture medium (10% FBS). After this time, the cells were collected by scraping in 1 ml of ice-cold phosphate-buffered saline (PBS) containing protease inhibitors (BIOMOL Research Laboratories, Plymouth Meeting, PA), and the nuclear fractions were separated from cytosolic fractions using a Nuclear/Cytosol fractionation kit (BioVision, Mountain View, CA), as indicated by the manufacturer. The cellular lysates were quantified by Bradford assays (Bio-Rad Laboratories, Hercules, CA) and 30 μg of proteins for each sample was separated on SDS-polyacrylamide gel electrophoresis (PAGE) for Western blot analysis with the reported antibodies.

ChIP. Endogenous FoxO3 or acetylated histone H3 (Lys9) were immunoprecipitated from soluble chromatin as described previously (Goruppi *et al*., 2007). Two sets of primers, amplifying the proximal and a distal FoxO binding regions (A and B, respectively), were used to amplify segments of the human *bnip3* promoter from the copurified DNA: Oligo A, GACACGACTGTCTGGGAAGC sense and CGTGGAGGCACTTTTCAGAG antisense; and oligo B, TGCGCCAGCATGTAATACTC sense and GAGGATGGGGCTTTGGTACT antisense. Parallel ChIPs were carried out using same amounts of affinity purified nonimmune rabbit antibodies (Cell Signaling Technology), and the associated DNA was amplified as a background control. An aliquot of total chromatin was amplified to determine the equal amount of chromatin used in each assay.

Immunoprecipitations and Immunoblotting

U2OS cells stable transfected with either green fluorescent protein (GFP) or GFPp8 were grown to confluence in 15-cm Petri dishes and either serum starved for 24 h or left untreated (10% FBS). The Western blots were performed as described previously (Goruppi *et al*., 2007). Expression levels were normalized to loading controls by using ImageJ software (http://rsb.info.nih.gov/ij/). Immunoprecipitation: Cells were recovered by gentle scraping in 1 ml of ice-cold PBS containing protease inhibitors (Calbiochem), and total cellular lysates were prepared as described in Goruppi *et al*. (2007). Immunoprecipitations were carried out using a mix of two anti-p8 antibodies (5 μg each) (Goruppi and Kyriakis, 2004) together with 10 μl of Ultralink Plus Protein A/G (Pierce Chemical, Rockford, IL), and the immunocomplexes washed three times in lysis buffer before SDS-PAGE and Western blot analysis with the indicated antibodies. Total proteins were normalized before immunoprecipitation.

Western Blots. Primary antibodies used include anti-LC3B, ATG12-5, caspase-3, cleaved caspase-3, cleaved rat caspase-9, poly(ADP-ribose) polymerase (PARP), cleaved PARP, Survivin, cIAP1, Sgk1, FoxO3, phosphorylated (p)-AMPKα, p-AMPKβ, p-S6, p-c-Jun NH_2-terminal kinase, and p-Akt from Cell Signaling Technology, and antibodies against p8, Bnip3, FoxO3, GFP, glutathione transferase (GST), Lamin A, tubulin, and actin were from Santa Cruz Biotechnology and Goruppi and Kyriakis (2004). Appropriate peroxidase-conjugated secondary were from Santa Cruz Biotechnology or Jackson ImmunoResearch laboratories (West Grove, PA), whereas enhanced chemiluminescence reagents were from Boston BioProducts (Ashland, MA).

Stable Red-LC3 Cell Line and Autophagy Detection

U2OS were transfected with pHcRed1-LC3, encoding for the far-red fluorescent protein (Clontech, Mountain View, CA) fused to LC3 and for neomycin resistance (kindly provided by Alessia Di Nardo, Harvard Medical School, Boston MA). The percentage of cells having Red-LC3 translocation into dots (a minimum of 100 cells/sample, in three separate experiments) was counted in the Red-LC3–expressing U2OS cells fixed at room temperature with 3.7% paraformaldehyde (Sigma-Aldrich, St. Louis, MO) in PBS, containing 10 μM Hoechst 33342 for nuclear staining. Cells with only nuclear Red-LC3 were considered negatives, whereas cells with more than five dots were considered as positive (Klionsky *et al*., 2008; Herrero-Martin *et al*., 2009). Cells with only cytosolic dots were considered positive (if >5).

U2OS Red-LC3 Stable Cells. Two days after transfection, the cells were divided and the following day they were selected using 0.5 mg/ml G418

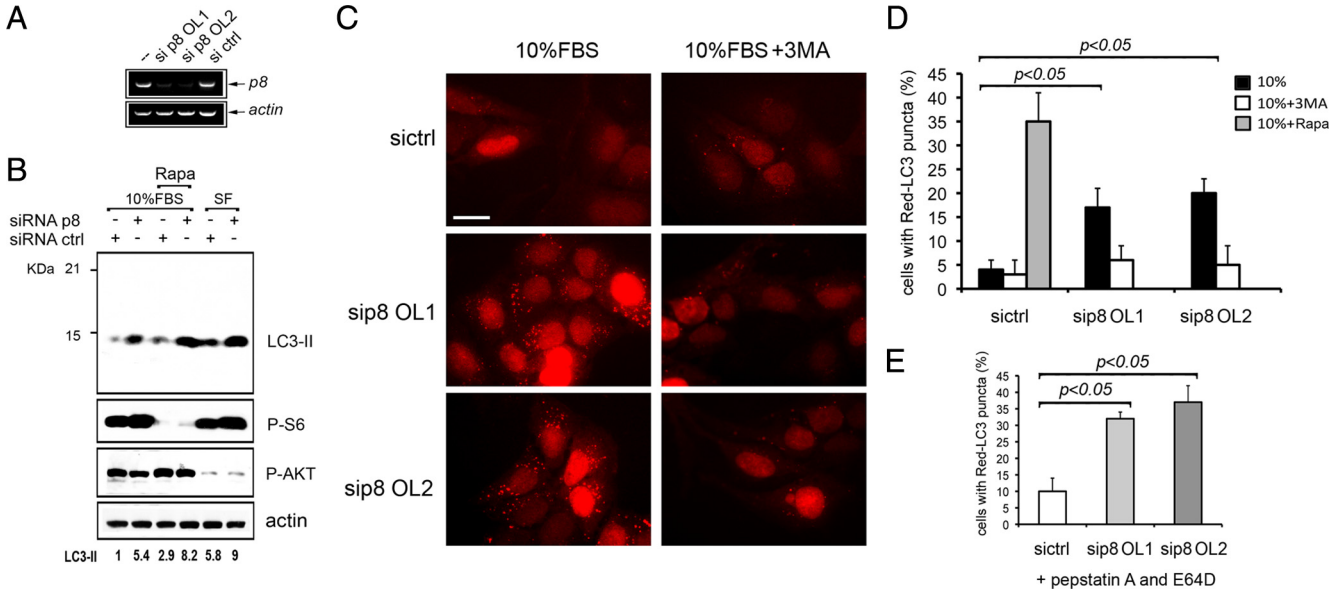

Figure 1. *p8* silencing causes an increase of autophagy. (A) *p8* RNAi in U2OS cells. Cells were transfected with two different *p8* siRNAs (OL1 and OL2) or with a mix of two nontargeting siRNA as control (ctrl). After 24 h total RNA was analyzed by RT-PCR, by using *p8*-specific and *actin*-specific oligonucleotides. (B) *p8* RNAi causes LC3-II processing in U2OS cells. Western blot analysis of total cellular lysates from U2OS cells after RNAi as described in A, and either left untreated or treated with 100 nM rapamycin (Rapa) or serum starved (SF) for additional 24 h. Membranes were developed using anti LC3B, p-S6, p-Akt, and actin antibodies. In this experiment, p-S6, p-Akt antibodies were used as treatment controls for serum starvation and Rapa addition. The LC3B antibody has a stronger reactivity for LC3B-II form. Film was quantitated by densitometry and fold induction of LC3-II, normalized to total actin, is shown. (C) *p8* silencing induces autophagosome formation in U2OS cells. Red-LC3–expressing U2OS cells after either OL1 or OL2 or *crtl* RNAi. The cells were fixed for the analysis after 48 h. When indicated, 10 mM 3MA or 100 nM rapamycin were added for 24 h. (C and D), Representative immunofluorescent images (63×; bar, 20 μm), and the percentage of cells with LC3 puncta is shown. (E) Percentage of cells with LC3 puncta in experiments as described in C and D having pepstatin A and E64D added for 4 h before analysis. The values represent the mean ± SEM for three experiments. Samples were subjected to unpaired Student's *t* test.

(Calbiochem) for 2 weeks. Several clones were expanded and selected by immunofluorescence for homogeneous recombinant protein expression. The autophagosome induction in the cell line was confirmed by rapamycin and Hanks' balanced salt solution treatment for 3 h. In the untreated U2OS cells, the Red-LC3 was nuclear or diffusely distributed in the cytosol, and only 2% of the cells presented dotted staining. The percentage was slightly increased (4–5%) in the cells transfected with control (crtl) siRNA (data not shown).

For immunocytochemical imaging, images were obtained using an E800 microscope (Nikon, Tokyo, Japan) coupled with a digital camera (Hamamatsu, Bridgewater, NJ). The software used was OpenLab 5 (PerkinElmer, Waltham, MA) on a Mac OS 10.5.6 platform. Mounting medium used for the images was Advantage permanent mounting media (Axell, Westbury, NY). Objectives used for image capture were 40× and 63× (Nikon). For the preparation of the figures, images were processed using Photoshop CS (Adobe Systems, Mountain View, CA).

Transient Transfection, DNA Constructs, and Luciferase Assays

Transfection methods, pEGFP, pEGFPp8, and pcDNA His5 p8 have been described previously (Goruppi and Kyriakis, 2004). The luciferase reporter containing six copies of FoxO binding site and wild-type FoxO3 have been described previously (Brunet *et al.*, 1999; Furuyama *et al.*, 2000). For analysis of p8 and FoxO3 transactivation activity, U2OS cells were transfected in triplicate using Lipofectamine 2000 reagent (Invitrogen, Carlsbad, CA), and the luciferase assays were carried out as described previously (Goruppi *et al.*, 2007). A plasmid encoding for β-galactosidase, pCMV βgal (5 ng/well), was coexpressed to normalize the transfection efficiencies.

Animal Experiments

p8 −/− mice and wild-type, *p8* +/+, littermate controls in C57BL/6J background have been described previously (Vasseur *et al.*, 2002b). Ten- to 12-week-old age-matched animals were analyzed in the study, and the hearts were removed under deep anesthesia. For echocardiography, mice were imaged in the left lateral decubitus position by using a Phillips-Sonos 7500 echocardiography system equipped with 11-MHz sector array and 10- to 15-MHz linear array transducers. Digital echocardiographic images were analyzed with Phillips-based analysis software (qLAB) on XP-based platform coupled with the echocardiography system. Left ventricular end-diastolic diameter (LVEDD) and left ventricular end-systolic diameter (LVESD) were measured and fractional shortening (FS) was calculated as (LVEDD − LVESD/LVEDD) × 100%. All studies and analysis were made by investigators blinded to mice genotype. All procedures were performed according to the animal protocol approved by Tufts University Animal Care and Use Committee.

Statistical Analysis

Independent experiments were pooled when the coefficient of variance could be assumed to be equal. Statistical significance was evaluated with Prism 5.0 software (GraphPad Software, San Diego, CA) by using nonpaired, two-tailed student's *t* test (n is number of experiments or animals analyzed). p values below 0.05 were considered significant and if lower are indicated.

RESULTS

p8 Silencing Increases Autophagy

To determine whether p8 plays a role in autophagy, we used siRNA-mediated silencing to knock down U2OS cell *p8* expression. Two sequences targeting human *p8* were used, OL1 and OL2, with both oligonucleotides completely silencing *p8* expression to a similar extent after 24 h, as detected by RT-PCR (Figure 1A). Serum starvation and inhibition of mTOR by rapamycin are known inducers of autophagy (Klionsky *et al.*, 2008); we thus asked whether p8 could affect autophagy induced by these stimuli. LC3 is a key component of autophagic complex, and LC3-I to LC3-II processing is a prominent marker for autophagy (Klionsky *et al.*, 2008). After *p8* or *ctrl* RNAi, U2OS cells were either maintained for 48 h in complete medium (10% FBS) or autophagy was induced by addition of 100 nM rapamycin (Rapa) or by serum starvation (SF) for 16 h.

Silencing of *p8* strongly stimulated LC3-II formation, even in medium containing 10% serum—a condition that should not provoke autophagy (Figure 1B and Supplemental Figure 1, A and B). Rapamycin or serum starvation each induced a strong up-regulation of LC3-II, but this induction was consistently higher after *p8* RNAi (Figure 1B). Thus, *p8* silencing induces LC3-II processing, indicating activation of autophagy.

The formation of LC3-II is associated with the aggregation of LC3-I in the autophagosomes. This aggregated LC3-II appears as puncta detectable by cytochemical methods. A fluorescent protein fused to LC3 is commonly used as an alternative approach to analyze autophagy (Klionsky *et al*., 2008). We thus established a U2OS cell line expressing the LC3 fused to a far-red fluorescent protein, Red-LC3 (Figure 1C). U2OS Red-LC3 cells were subjected to *p8* RNAi by using either OL1 or OL2 (Figure 1A), and 3-methyl adenine (3MA), an inhibitor of autophagy was used in parallel experiments (Figure 1D). As positive control, after *ctrl* RNAi, Red-LC3 cells were treated with 100 nM rapamycin. In all the experiments, cells were visualized by nuclear Hoechst staining, and the percentage of cells bearing at least five puncta was quantitated, as described in Klionsky *et al*. (20080 and Herrero-Martin *et al*. (2009). Consistent with Figure 1B, *p8* silencing leads to autophagosomes accumulation with at least 20% of the cells manifesting autophagic puncta. The appearance of puncta was inhibited by 3MA addition (Figure 1, C and D). When E64D and pepstatin were added for 4 h before the analysis, we found a similar higher percentage of Red-LC3–positive cells after *p8* silencing, strongly suggesting an increase of the "on rate" of the autophagic process (Figure 1E). Thus, our data indicate that silencing of *p8* is sufficient to increase the basal autophagosome formation in U2OS cells and is blocked by autophagy inhibitors incubation.

p8 Protects from Autophagy-induced Apoptosis

Autophagy can be either protective or deleterious on cellular fate (Maiuri *et al*., 2007). We thus set out to determine the effects of *p8* RNAi on cellular viability and consequent to autophagy activation by serum starvation, AMPK stimulation with AICAR, or by mTOR inhibition with rapamycin. Thus, after *p8* RNAi we applied autophagic stimuli and assessed cell viability by MTT assays. Silencing of *p8* decreased the survival of cells cultured in the presence of 10% FBS (Figure 2A) and enhanced cell death to an even greater degree upon activation of autophagy by serum starvation, AICAR, or rapamycin (Figure 2, A and B). The effects of *p8* RNAi on cell death provoked by serum depletion were reversed when cells were simultaneously treated with autophagy inhibitor 3MA (Figure 2B). These findings were confirmed in assays with U87MG cells, a glioblastoma cell line (Supplemental Figure 1, B and C). In parallel experiments, we monitored autophagy levels in the same conditions as in Figure 2B (Figure 2C). A further increase of LC3-II upon pharmacological activation of autophagy in serum starved cells was detected and was blocked by 3MA addition (Figure 2C). On line with this evidence, 96 h of *p8* RNAi resulted in a decrease in total U2OS cell number, as quantified by direct cell count and consistent with an effect on cellular viability (Figure 2D).

We further analyzed the mechanism responsible for autophagy induction by *p8* RNAi. As for cellular viability (Figure 2B), the addition of 3MA to the cell medium suppressed the increase in LC3-II upon *p8* RNAi (Figure 2E). The enhancement, by *p8* RNAi, of serum starvation-induced cell death may be due to the disruption of intracellular energy balance as methylpyruvate, a growth factor-independent energy source, reversed the *p8*-dependent increase of LC3-II processing (Figure 2E). Thus, p8 seems to suppress autophagy and cell death associated with autophagic stimuli, rendering cells less sensitive to energy stressors.

We further assessed whether the decrease in cell viability observed after *p8* silencing was due to apoptotic cell death. To this end, we analyzed targets of caspase machinery and found that *p8* siRNA triggered both nuclear PARP cleavage and a decrease in total caspase-3, indicative of its processing. Accordingly, we observed a decrease in the caspase-3 inhibitor survivin, whereas no significant changes for c-IAP1 were found (Figure 2F).

To determine whether blocking apoptosis had an effect on autophagy, we performed an experiment where *ctrl*- and *p8*-silenced U2OS cells were treated with the caspase inhibitor zVADfmk (ZVAD) and, as positive control, simultaneously with ZVAD and autophagy inhibitor 3MA. The effects on autophagy and apoptosis were monitored with LC3B, cleaved PARP and total caspase-3 antibodies. We found that ZVAD treatment did not affect *p8* silencing-induced LC3 processing, but, as expected, it blocked PARP cleavage. Addition of both ZVAD and 3MA abolished both autophagy and apoptosis (Figure 2G). Together, the results in Figure 2 indicate that the presence of *p8* protects cells from autophagy and that *p8* silencing provokes autophagy and cell death associated with caspase activation.

p8 Represses FoxO3 Transactivation

We next sought to identify the mechanisms by which p8 regulates autophagy. We have shown that p8 is a cotranscriptional regulator in cardiovascular and cancer cells (Goruppi *et al*., 2007). In many instances, the induction of autophagy is accompanied by the expression of a number of genes (Attaix and Bechet, 2007; Klionsky *et al*., 2008). Thus, we asked whether p8 might regulate the induction of autophagy via a transcriptional mechanism. The transcription factor FoxO3 has been reported to control autophagy (Mammucari *et al*., 2007; Zhao *et al*., 2007). We used a FoxO luciferase reporter to test the effects of p8 expression on FoxO3 transactivation. We found that p8 coexpression triggered a complete repression of the FoxO3-dependent reporter transactivation ($p <$ 001) (Figure 3A). Likewise, expression of a GFP-tagged p8 had no significant reporter activity and, when coexpressed, inhibited the FoxO3 reporter transactivation (Figure 3A). When FoxO3 was expressed with decreasing concentrations of p8 a dose dependent derepression was detected, ruling out the possibility of a toxic effect due to protein overexpression (Figure 3B).

In the presence of serum, FoxO3 is kept inactive and sequestered in the cytosol through a phosphatidylinositol 3-kinase/Akt-dependent mechanism. On serum withdrawal, FoxO3 enters the nucleus and becomes active (Brunet *et al*., 1999). To determine whether *p8* expression might interfere with FoxO3 intracellular localization, we generated a U2OS cell line in which *p8* was silenced by lentiviral short hairpin RNA (shRNA) (LV sip8), and control cells were generated by infecting with empty shRNA lentiviruses (LV sictrl) (Supplemental Figure 2B). Nuclear and cytosolic extracts were prepared and FoxO3 detected on immunoblots. SGK1 and Lamin A provided cytosolic and nuclear markers, respectively (Figure 3C). The levels of FoxO3 were quantified and expressed as the nuclear (N) to cytoplasmic (C) ratio. We found that cells in which *p8* expression was silenced had significantly higher levels of nuclear FoxO3 even in presence of serum (0.5 ± 2 vs. 1.7 ± 5, respectively; $p < 0.05$; $n = 3$), indicative of a possible functional interaction between FoxO3 and p8 (Figure 3C). No change in total FoxO3 protein expression was detected in total cellular lysates made in SDS-loading buffer (Figure 3C, middle).

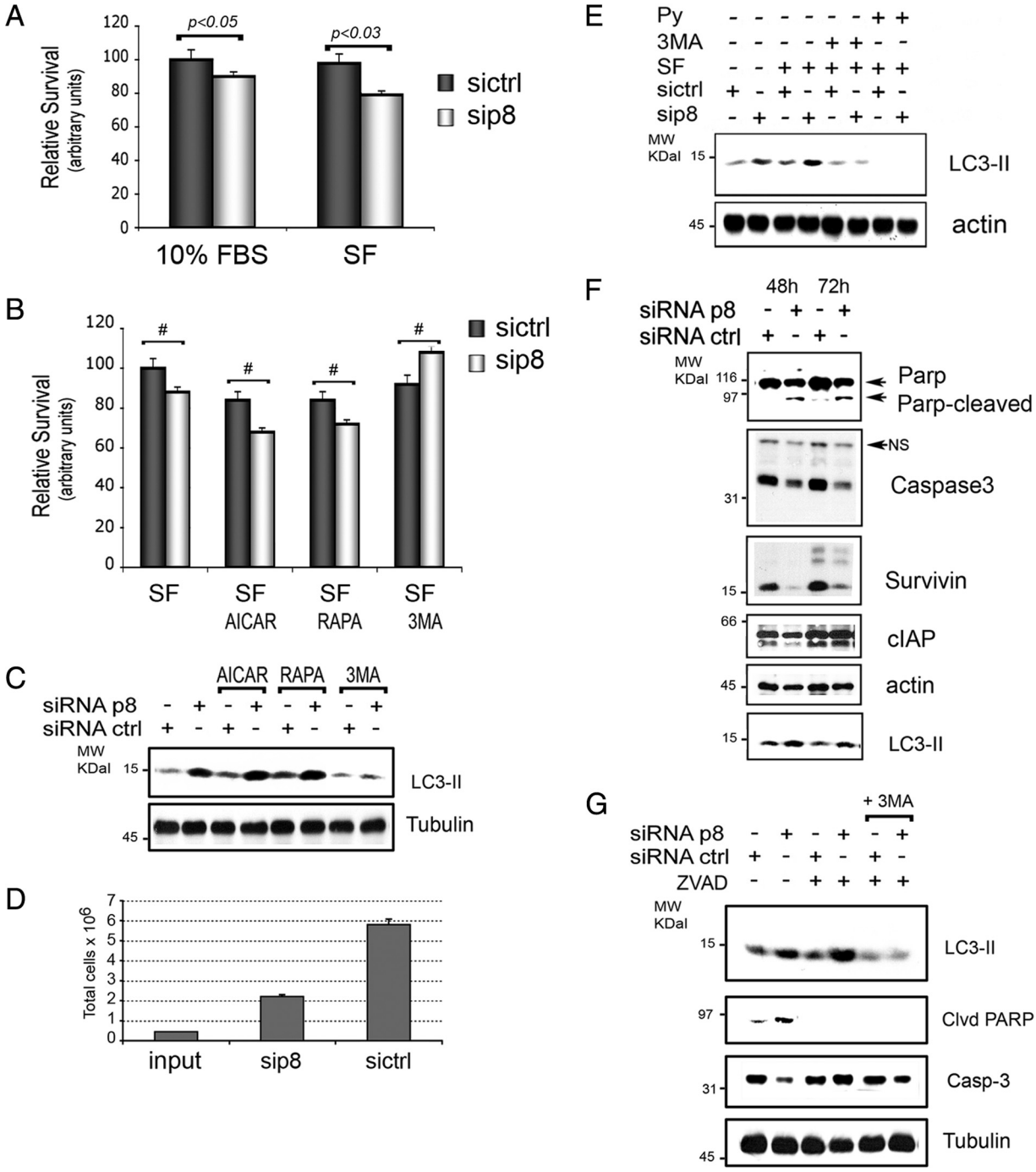

Figure 2. *p8* presence protects from autophagy-induced apoptosis. (A–C) *p8* RNAi decreases cellular viability in response to autophagy stimuli. U2OS were cultured for 48 h after *p8* or *ctrl* RNAi, and then the cells were cultured for further 48 h with 10% FBS or without FBS (SF) before cell viability assays. When indicated, 1 mM AICAR (AICAR) or 100 nM rapamycin (RAPA) or 10 mM 3MA was added. (B) Values were normalized to *ctrl*-silenced cells in serum-free conditions. Values represent the mean ± SEM for five experiments in triplicate. Samples were subjected to unpaired Student's *t* test. #$p < 0.05$. (C) Western blot analysis of the levels of LC3-II in total cellular lysates of U2OS treated as described in B. (D) Decrease of total cell number following *p8* RNAi. U2OS were cultured for 96 h after *p8* (sip8) or *ctrl* (sictrl) RNAi, and cell number was evaluated using a hemocytometer. The values represent the mean ± SEM for three experiments. (F) *p8* RNAi-induced LC3 processing is blocked by autophagy inhibitors. Western blot analysis after *p8* or *ctrl* RNAi as described in Figure 1A and serum starvation (SF) or treatment with 10 mM 3MA or 10 mM methylpyruvate (Py) for 24 h. Western blots were performed with anti-LC3B and actin antibodies. (E) *p8* RNAi induces autophagy and concomitant apoptosis in U2OS cells. U2OS were cultured in 10% FBS for 48 and 72 h after *p8* (sip8) or *ctrl* (sictrl) RNAi. Total cellular lysates were analyzed with antibodies to autophagy, survival, and apoptosis markers, as indicated. Actin was used to normalize the loading. Representative Western blots are shown. (G) *p8* RNAi-induced LC3 processing is not blocked by apoptosis inhibitors. Analysis after *p8* or *ctrl* RNAi as in Figure 1A and treatment with 20 μM zVADfmk (ZVAD) caspase inhibitor alone or with ZVAD and 10 mM 3MA combined for 16 h in 10% FBS. The Western blots were carried out with LC3B, caspase-3, cleaved PARP, and tubulin antibodies.

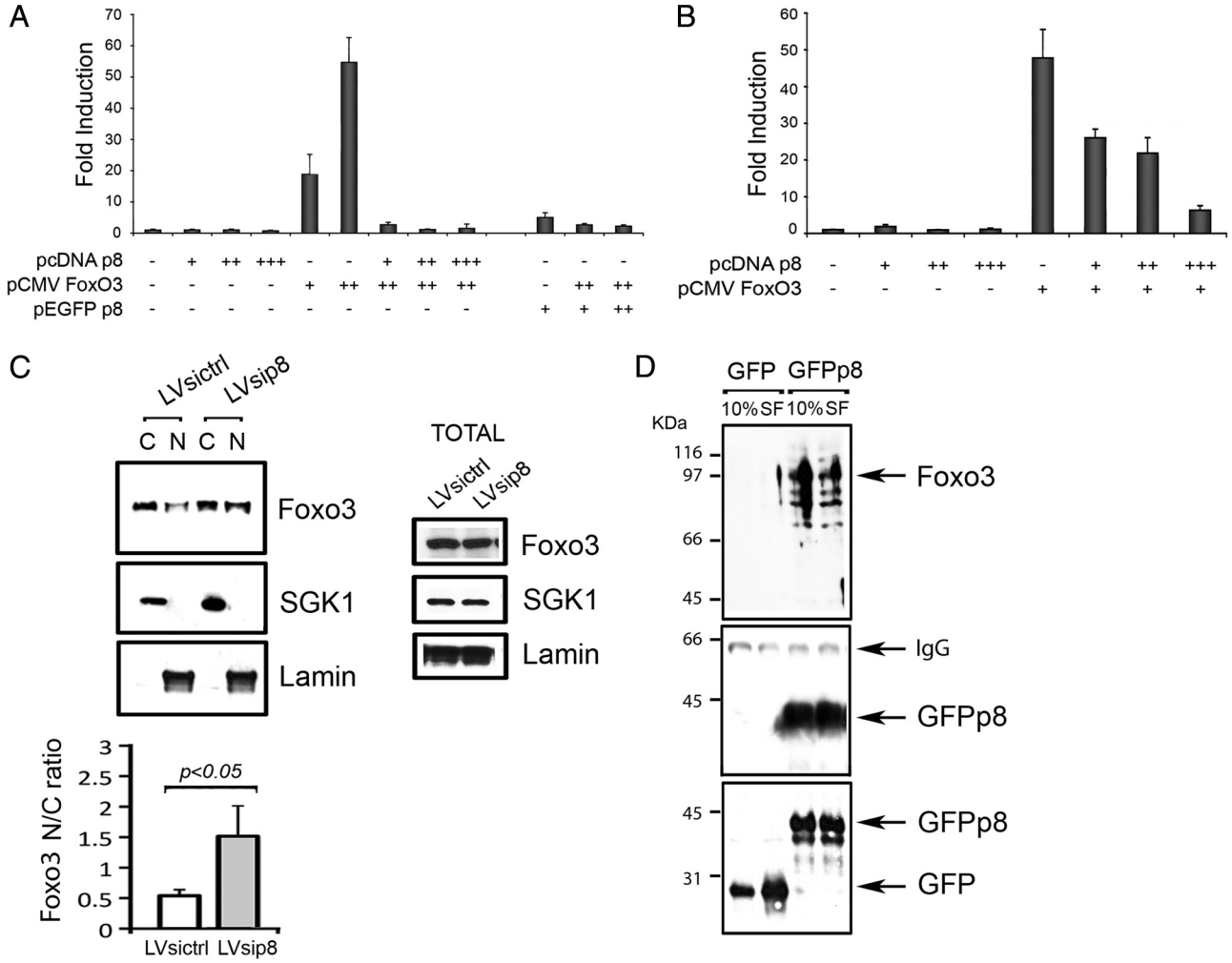

Figure 3. p8 interacts with and represses Foxo3 transactivation. (A and B) p8 represses FoxO3 transactivation in a dose dependent manner. U2OS cells were transfected with a FoxO transcription factors reporter and a combination of pcDNAp8, pEGFPp8, and pCMVFoxO3 wild type (wt). The next day, cells were serum starved (0.1% FBS) for 16 h. Luciferase activity was measured in triplicate and normalized to β-galactosidase activity. The FoxO3 concentration having maximal transactivation was cotransfected with increasing amounts of pcDNAp8, in B. Mean ± SEM for four experiments is shown. (C) U2OS cells were infected either with a control silencing lentivirus (LV sicrtl) or a lentivirus silencing human *p8* (LV sip8). Confluent cells were subjected to nuclear/cytosolic separation (N and C). The Western blots were carried out with the indicated antibodies, quantitated by densitometry, and the normalized values are indicated as nuclear/cytosol ratio in the histograms (mean ± SEM for three experiments; $p < 0.05$). Separate cultures were analyzed for total protein expression (right). (D) p8 binds to endogenous FoxO3. U2OS cells expressing enhanced green fluorescent protein (EGFP) or EGFPp8 were either left untreated (10%) or serum starved (SF) for 24 h before immunoprecipitation with anti-p8 antibodies. The western blots were carried out with anti-FoxO3 and p8, whereas total lysates were stained with GFP.

To investigate whether the observed increase in nuclear FoxO3 localization in *p8* knockdown cells might be a consequence of a direct interaction with p8, we performed immunoprecipitations from U2OS expressing either GFP or GFPp8 (Supplemental Figure 2A) by using anti-p8 antibodies. FoxO3 was clearly detected in cells expressing p8 and the interaction was not apparently influenced if the cells were serum starved for 24 h (Figure 3D). Altogether, our results indicate that p8 expression is able to repress FoxO3-dependent transactivation in U2OS cells and that *p8* knockdown increases nuclear FoxO3.

p8 Suppresses FoxO3 Association with the bnip3 Promoter and Modulates bnip3 RNA and Protein Levels in U2OS Cells

The above-mentioned studies suggested that p8 might regulate FoxO3-dependent induction of autophagic genes. The promoters of several autophagy genes (*lc3*, *bnip3*, and *atg12*) contain multiple FoxO consensus *cis*-acting sequences (Mammucari *et al*., 2007; Zhao *et al*., 2007). We focused on Bnip3, a protein whose inhibition blocks autophagy in cardiomyocytes and hypoxic tumors, whereas if overexpressed it can induce autophagy and repress mTORC1 (Hamacher-Brady *et al*., 2006; Hamacher-Brady *et al*., 2007; Li *et al*., 2007). Several studies suggest a major role for Bnip3 in FoxO3-induced autophagy in vitro and in vivo (Mammucari *et al*., 2007; Zhang and Ney, 2009).

We tested the effects of *p8* RNAi on FoxO3's association with two different regions on the *bnip3* promoter (A and B in Figure 4A). After *p8* or control RNAi treatment, U2OS cells were either left in presence of serum or serum starved for 20 h before performing ChIPs. DNA Copurified with FoxO3 and NRS ChIPs were amplified by PCR using the oligonucleotide surrounding sequences A and B (Figure 4A). We

found that silencing of *p8* increases the association of FoxO3 with chromatin containing the *bnip3* promoter. Along with the results in Figure 3A, these data suggest that p8 negatively regulates FoxO3 transactivation of *bnip3*. Accordingly, *p8* silencing also increased the levels of Bnip3 mRNA, as detected by RT-PCR (Figure 4B). Moreover, when separate ChIPs were performed using acetylated-histone H3 (Lys9) antibodies, which recognize transcriptionally active chromatin, we found that *p8* RNAi increases the levels of chromatin containing acetylated histone H3. These data suggest that in situ p8 reduces the level of active chromatin (Figure 4A). In accordance with our RNA and ChIP studies, we found that Bnip3 protein levels are increased upon *p8* silencing (Figure 4C).

We next examined whether *bnip3* expression was responsible for the decrease in viability after *p8* silencing. To this end, we either silenced *p8* or both *bnip3* and *p8*, before inducing autophagy for 48 h, as in Figure 2. We found that although *p8* silencing alone impaired cellular viability, concomitant silencing of *p8* and *bnip3* restored the cellular viability both in the presence or the absence of serum (Figure 4D).

We further investigated the effects on cell survival of simultaneous *p8* and autophagy knockdown by silencing the essential component of the autophagic machinery *atg5* (Klionsky *et al*., 2008). To this end, we either silenced *p8*, *atg5*, and *bnip3* alone or in combination before serum starvation for 48 h (Figure 4E and Supplemental Figure 2C). We found that simultaneous silencing of *atg5* and *p8* blocked LC3 processing and decreased apoptosis, as detected by PARP cleavage and total caspase3 levels (Figure 4E). *Bnip3* and *p8* silencing blocked apoptosis, but a higher basal LC3 processing was still detectable. From Figure 4, A–E, we can conclude that *p8* silencing up-regulates Bnip3 and causes ATG5-dependent autophagy and Bnip3-dependent apoptosis. Interestingly, in absence of apoptosis, higher levels of LC3-II were detected in *bnip3* and *p8* cosilenced cells (Figure 4E). Together, our results in Figures 3, A–C and 4, A–E, indicate that p8 suppresses the association of FoxO3 with the *bnip3* promoter and that *p8* absence increases *bnip3* transcription and protein levels. More importantly, Bnip3 seems to be a key target mediating cell death induced by *p8* silencing.

Cellular Energy Stress Acts on p8 Expression and Stability

Metabolic stress results in a decrease in ATP and an accumulation of AMP, which activates AMPK (Hardie, 2007). Likewise, amino acid depletion deactivates mTORC1, resulting in reduced protein synthesis (Meijer and Codogno, 2008). To determine whether metabolic stresses could act on p8 expression, we induced autophagy in U2OS cells with AICAR and followed p8 protein levels over time. The expression of endogenous Bnip3 and the induction of LC3-II were monitored in parallel. As controls, we followed the levels of AMPK activation and the induction of apoptosis. We found that endogenous p8 protein was transiently induced between 1 and 9 h after AICAR addition. Induction of autophagy by AICAR was associated by a slight increase of total Bnip3 protein (Figure 5A). After 16 h, endogenous p8 levels were down-regulated and concomitantly the induction of Bnip3 was up-regulated, as were LC3-II levels. Endogenous p8 stabilization by AICAR was transient. Accordingly, both amino acid and glucose starvation stabilized p8 in primary rat cardiomyocytes (Supplemental Figure 3, A and B). AMPK phosphorylation was first detected at 1 h from AICAR addition and remained higher than basal at later time points, when PARP cleavage became evident (Figure 5A). Thus, although autophagic stimuli such as AICAR induce p8 transiently, markers of autophagy are fully up-regulated in AICAR-stimulated cells when p8 levels decline back to basal. These findings are consistent with our observations indicating that p8 suppresses autophagy by reducing the transcription of Bnip3.

We and others have reported that p8 polypeptide undergoes multiple posttranslational modifications, some of them required for its stabilization. Endothelin-1 and β-adrenergic agonists act at transcriptional level, whereas others, such as TNF, modify both expression and protein stability. In addition, p8 turnover is regulated by Akt-glycogen synthase kinase 3 signaling, which is sensitive to serum withdrawal (Goruppi and Kyriakis, 2004; Goruppi *et al*., 2007; Chowdhury *et al*., 2009; Goruppi and Iovanna, 2009). To determine whether the transient increase of endogenous p8 polypeptide is determined by signaling regulating the autophagic process, we transfected 293 cells with pcDNA p8 and treated them with either AICAR, 2DG, rapamycin, or TNF as positive control, both in presence of serum (10%) or under serum-free conditions. Immunoblotting with anti p8 antibodies showed that serum depletion increased p8 polypeptide levels modestly, whereas AICAR and 2DG stimulated robust increases in p8 protein, both under normal serum conditions and in serum-free conditions. Rapamycin did not affect p8 levels (Figure 5B). Thus p8 polypeptide stability is a target of AMPK-activated signaling but not of mTOR or serum withdrawal.

Because AICAR-induced autophagy is associated with endogenous Bnip3 up-regulation and a decrease in endogenous p8 levels (Figure 5A), we explored the effects of p8 overexpression on AICAR-induced Bnip3 up-regulation. To this end, we took advantage of U2OS cells expressing either GFP or GFPp8 (Figure 4D and Supplemental Figure 2A) and analyzed over time the levels of endogenous Bnip3 after AICAR addition. As in parental U2OS cells (Figure 5A), in GFP-expressing U2OS cells the basal Bnip3 levels were strongly up-regulated after 24 h from AICAR addition (Figure 5C). By contrast, and consistent with a p8 corepressor function, no significant endogenous Bnip3 up-regulation was detected in GFPp8-expressing U2OS cells (Figure 5C). Together these data suggest that, after a transient stabilization, the induction of autophagy by stimuli mimicking energy stress is associated with the down-regulation of endogenous p8, which leads to a concomitant up-regulation of endogenous Bnip3.

p8 Silencing Increases Autophagy and Apoptosis in Cardiac Cells

Our results in Figure 1 and 2 demonstrate that *p8* silencing in U2OS cells is followed by an increase in basal autophagy levels and apoptosis. We have reported previously that p8 is expressed in cardiac cells (Goruppi *et al*., 2007); we thus explored the consequences of *p8* silencing in primary neonatal rat cardiomyocytes and in rat H9C2 cardiomyoblast cells. We monitored the autophagy levels and apoptosis 72 h after either *ctrl* or *p8* RNAi (Goruppi *et al*., 2007). In both cardiomyocytes and H9C2 cells, we studied the effects of *p8* silencing in the presence or absence of lysosome inhibitors (E64D and pepstatin) and in H9C2 cells also in presence/absence of the autophagy inhibitor (3MA). The induction of autophagy was detected with LC3B antibodies and the activation of apoptosis was monitored with caspase-3, caspase-9, and PARP antibodies by Western blot. We found that silencing of *p8* resulted in LC3 processing in both cardiomyocytes and H9C2 cells, which was dramatically increased by the lysosomal inhibitors, thus ruling out LC3-II flux as an explanation for increased LC3-II levels after *p8* RNAi (Figure 6, A–C). This was correlated with a significant apoptosis in both cardiac cells (Figure 6,

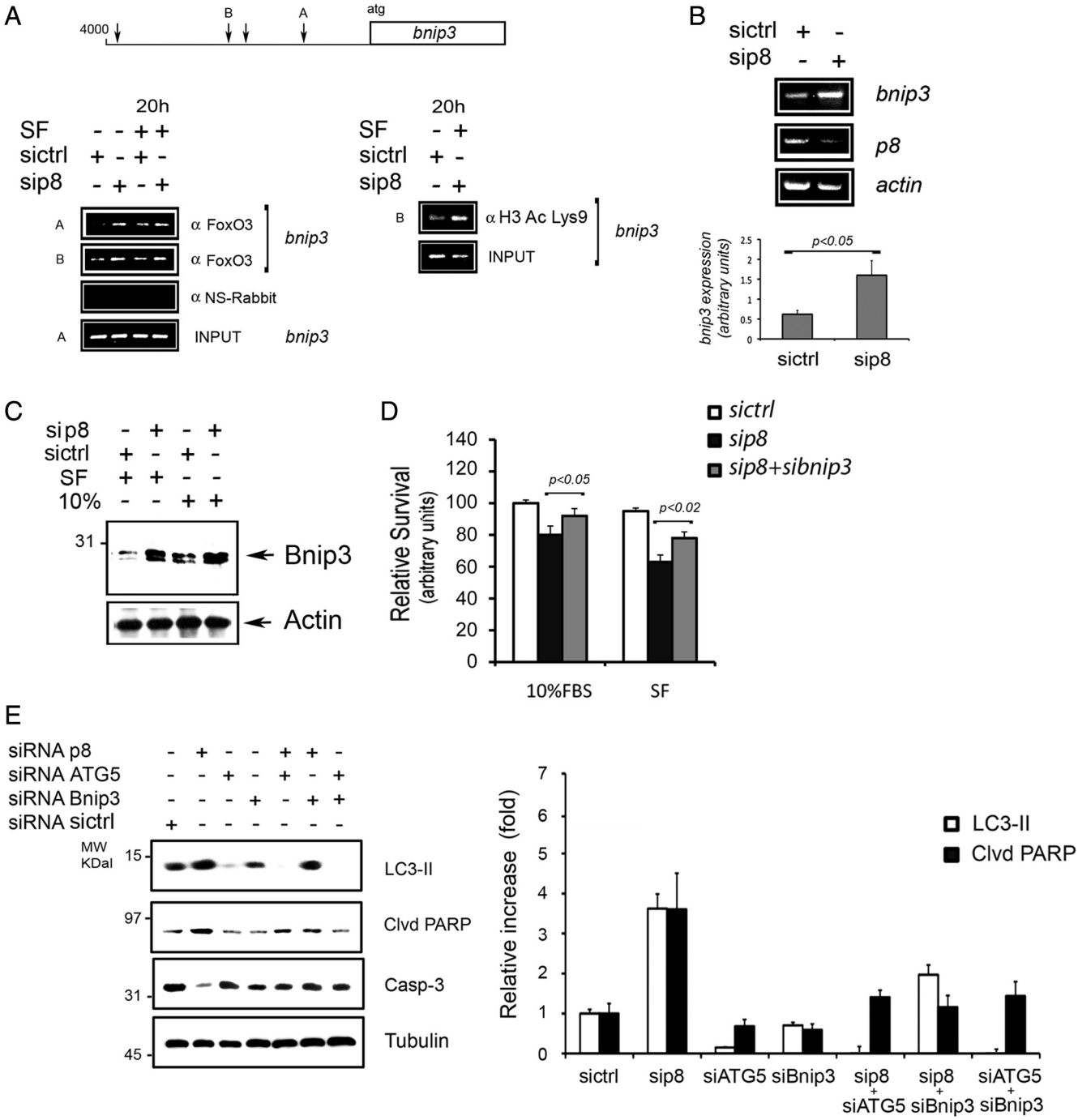

Figure 4. *p8* RNAi increases FoxO3 association to *bnip3* promoter resulting in higher *bnip3* RNA and protein levels. (A) Increased FoxO3 association to endogenous *bnip3* promoter after *p8* RNAi. U2OS 24 h after *p8* or *crtl* RNAi were either left untreated or serum starved (SF) for additional 20 h before harvesting. Chromatin immunoprecipitations of endogenous FoxO3: either anti FoxO3 (αFoxO3) or a nonimmune serum (αNS-Rabbit) were used. Total cellular chromatin (INPUT). Two FoxO-responsive elements in the *bnip3* promoter (A and B in the *bnip3* promoter scheme) were analyzed. *p8* RNAi increases histone H3 acetylation on *bnip3* promoter. ChIPs were performed from U2OS chromatin by using anti-lysine 9-acetylated histone H3 antibodies. PCR reactions were made using B oligonucleotides. (B) *p8* RNAi enhances *bnip3* RNA expression. U2OS were treated as described in Figure 2A, and RT-PCRs were run using *bnip3*, *p8*, and *actin* oligonucleotides. The histograms show the mean values ± SEM for three experiments. $p < 0.05$. (C) *p8* RNAi increases Bnip3 protein levels. Western blot analysis of total cellular lysates from U2OS cells treated as described in Figure 5A, using either anti Bnip3 or actin antibodies, as loading control. (D) Knockdown of *bnip3* decreases cell death associated with *p8* silencing. U2OS were cultured for 48 h after *ctrl*, *p8* alone, or *p8* and *bnip3* RNAi. Cellular viability assays (MTT) were performed after additional 48 h. The values represent the mean ± SEM for three experiments in triplicate. Samples were subjected to unpaired Student's *t* test. (E) *p8* RNAi induces *atg5*-dependent autophagy and *bnip3*-dependent apoptosis. U2OS were cultured for 48 h in serum-free after *ctrl*, *atg5*, *p8*, and *bnip3* alone or after combined *p8*+*atg5*, *p8*+*bnip3*, and *atg5*+*bnip3* RNAi. Western blot analysis of total cellular lysates using LC3B, anti-cleaved PARP, caspase-3, and tubulin antibodies. The efficiency of *atg5* and *bnip3* knockdown is shown in Supplemental Figure 2C. The quantification of two separate Western blots is shown on the right.

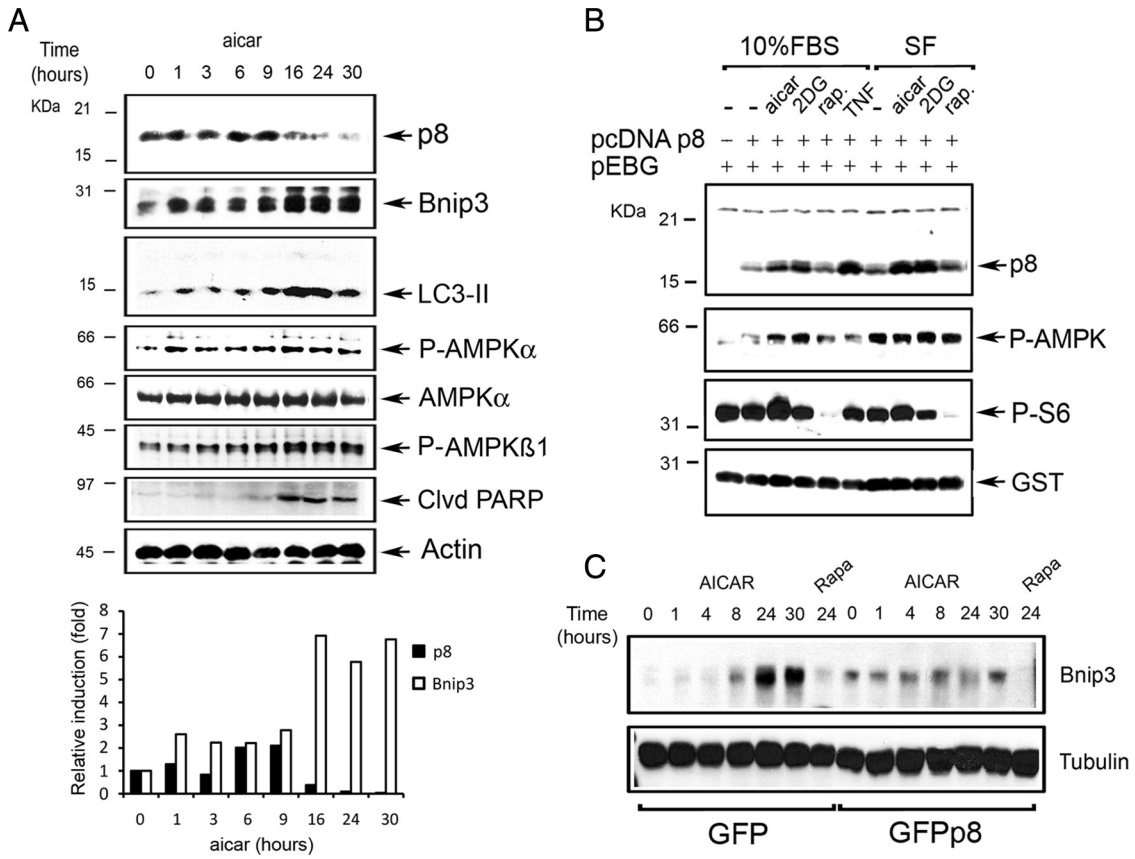

Figure 5. Cellular energy stress acts on p8 expression and stability. (A) Endogenous *p8* is down-regulated by AMPK-signaling in U2OS cells. Analysis of U2OS cells stimulated for the indicated times with 1 mM AICAR. The Western blots were carried out with anti-p8, Bnip3, LC3B, p-AMPKα, p-AMPKβ, AMPK-cleaved PARP, and actin antibodies. For p8 and Bnip3, values were quantified as fold of induction relative to the untreated cells levels. (B) Ectopic expressed *p8* is stabilized by 2DG and AICAR. 293 cells were cotransfected with pcDNAp8 and a vector expressing GST protein (pEGB). After 2 d, the cells were treated for 8 h with 20 mM 2DG, 1 mM AICAR, 20 ng/ml rapamycin, and 20 ng/ml TNF (positive control) either in the presence (10% FBS) or absence (SF) of serum in the culture medium. The Western blot analysis of total lysates was performed using anti-p8, anti-p-AMPK, p-S6, and GST as treatments and efficiency of transfection controls, respectively. (C) *p8* overexpression blocks endogenous *Bnip3* up-regulation by AICAR. Analysis of EGFP- or EGFPp8-expressing cells stimulated for the indicated times with AICAR as described in A. The Western blots were made with anti-Bnip3 and tubulin antibodies.

A–C) and was blocked by 3MA addition in H9C2 cells (Figure 6C). Three results are consistent with our evidence in U2OS cells and show an increase of 3MA-dependent autophagy after *p8* silencing in cardiomyocytes, which is associated with caspase activation.

To further support our findings in the cardiovascular system, we investigated the effects of p8 expression on FoxO3-dependent transactivation. As for the U2OS cells (Figure 3, A and B), we found that p8 coexpression in the H9C2 cardiac cell line resulted in a repression of the FoxO3-dependent reporter transactivation (Figure 6D). Likewise, when FoxO3 was expressed with increasing concentrations of p8, a dose-dependent repression was detected (Figure 6D).

In addition to cardiomyocytes, several different cell types can be found in the human heart (Rothermel and Hill, 2008b). We thus explored whether a similar increase in basal autophagy levels after *p8* silencing, as detected in cardiomyocytes, occurred in primary human cardiac fibroblasts (hCFs) and in primary human aortic endothelial cells (HAECs). In both primary human cell types, *p8* silencing for 72 h was associated with an increase of basal LC3 processing (Figure 5D). These studies strengthen our findings in U2OS cells and extend their relevance to the cardiovascular system.

Cardiac Tissue from p8 −/− Mice Exhibits Higher Basal Autophagy

We have shown that p8 plays a crucial role in regulation of cardiomyocyte hypertrophy and cardiac fibroblast production of MMPs, suggesting a function for p8 in the heart (Goruppi *et al*., 2007). We took advantage of *p8 −/−* mice to investigate whether disruption of *p8* is associated with increased autophagy in the heart. RT-PCR confirmed the expression of *p8* in the left ventricles (LVs) of wild-type (*p8 +/+*) mice, and, as expected, its absence in *p8 −/−* mice (Figure 7A). We analyzed by Western blot the levels of LC3-II and Atg12–5 in the LV total lysates of age-matched *p8 +/+* and *p8 −/−* mice. We found that disruption of *p8* led to significantly elevated levels of LC3-I and LC3-II, and of Atg12–5 ($p < 0.03$, $n = 5$ and $p < 0.02$, $n = 5$, respectively), indicating a greater basal autophagy (Figure 7B). The increase in LC3-I and LC3-II observed was not apparently due to a direct transcriptional effect, because we detected no significant difference in *lc3* mRNA between *p8 −/−* and *p8 +/+* mice (Figure 7C), by RT-PCR. Consistent with our RNAi and overexpression results, we found that both RNA and protein expression of *bnip3* were higher in p8 −/− ($p < 0.01$, $n = 6$ and $p < 0.05$, $n = 4$, respectively) (Figure 7, C and

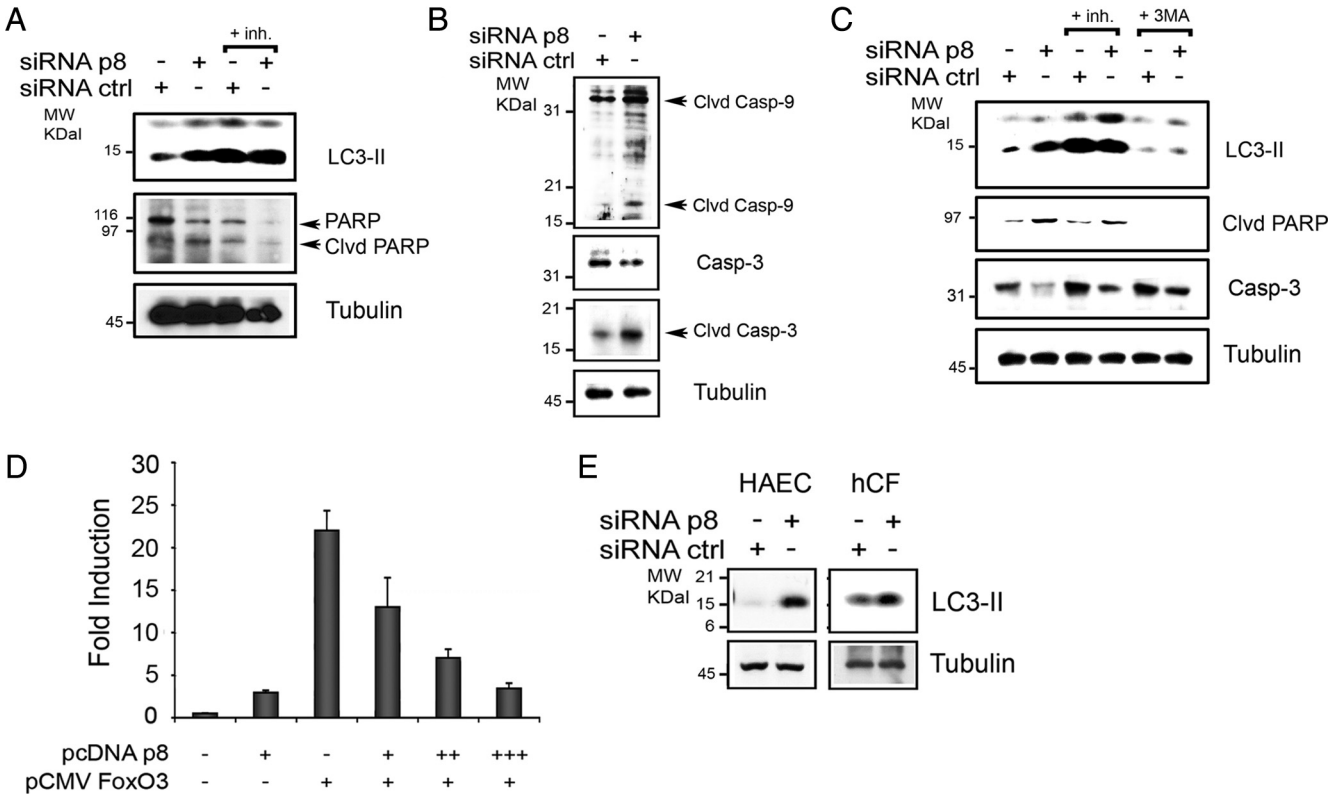

Figure 6. *p8* silencing in cardiovascular cells. (A–C) *p8* silencing increases autophagy and apoptosis in cardiac cells. *p8* RNAi in primary neonatal rat cardiomyocytes (A and B) and in rat H9C2 cardiac cells (C). Cells were cultured for 72 h in 10% FBS after (rat) *p8* or *ctrl* RNAi. When indicated, both pepstatin A and E64D were added for 4 h (+inh) or 10 mM 3-methyladenine (+3MA) was added for 16 h before analysis. The Western blots were performed with anti-LC3B, PARP, rat-specific cleaved (clvd) caspase-9, and total and cleaved (clvd) caspase-3 antibodies for cardiomyocytes and LC3B and cleaved (clvd) PARP and caspase-3 antibodies for H9C2 cells. Tubulin was used as loading control. (D) p8 represses FoxO3 transactivation in a dose-dependent manner in H9C2 cells. H9C2 cells were transfected in triplicate with a FoxO luciferase reporter and pcDNAp8 and pCMVFoxO3 wt as described for Figure 3A). In separate experiments, FoxO3 was cotransfected with increasing amounts of pcDNAp8. Luciferase activity was measured in triplicate and normalized to coexpressed β-galactosidase activity. Means ± SEM for two experiments are shown. (E) *p8* silencing increases autophagy in primary human cells. *p8* RNAi in primary hCFs and in primary HAECs. Cells were cultured for 72 h in 10% FBS after *p8* or *ctrl* RNAi, and the Western blot analysis was performed as described in A.

D). These findings indicate that, as with silencing of *p8* in cultured cells, the disruption of *p8* is associated with an increase in the expression of autophagy markers also in vivo.

p8 Genetic Deletion Is Associated with a Cardiac Phenotype

Autophagy in the heart under baseline conditions is a homeostatic mechanism for the maintenance of normal cardiac function and morphology. However, unrestrained or excessive autophagic activity can result in cardiac cellular loss and cardiac dysfunction (De Meyer and Martinet, 2008; Kundu and Thompson, 2008; Rothermel and Hill, 2008a). We have shown previously that p8 is induced in human failing hearts and by stimuli associated with cardiac remodeling (Goruppi *et al*., 2007). To determine whether *p8* genetic deletion was associated with a change in heart function, we performed echocardiographic recordings of *p8* +/+ (n = 15) and p8 −/− (n = 16) mice and measured their left ventricle wall dimensions and ventricle performance. We found that compared with their *p8* +/+ littermates, the *p8* −/− mice present a small but significant LV dilation ($p < 0.05$), as detected by end-diastolic and end-systolic dimensions (Figure 8A), which result in a lower fractional shortening ($p < 0.01$) (Figure 8C). In addition, compared with *p8* +/+ mice, *p8* −/− mice develop a LV posterior wall thinning ($p < 0.05$), whereas no significant differences were found for the LV anterior wall (Figure 8B). Our findings indicate that in vivo *p8* absence causes an increase in *bnip3* proautophagic gene expression associated with an increase of autophagic markers. In the heart, in vivo *p8* deletion results in a decreased cardiac functionality.

DISCUSSION

Autophagy has been implicated in the pathogenesis of various diseases, including cancer, neurodegeneration, and cardiomyopathies. Central to the discussion of autophagy in disease pathogenesis is its role in adapting to cellular stress versus its role in contributing to cell death (Maiuri *et al*., 2007; Mizushima *et al*., 2008; Rothermel and Hill, 2008a). Multiple stimuli induce autophagy in mammalian cells; and although there is evidence for a transcriptional regulation, the mechanisms involved in this process are still poorly understood. The present study unveils a role for p8 in autophagy control and provides new insights into the mechanisms by which FoxO3 regulates autophagy. In particular, we show that in vitro and in vivo p8 depletion is associated with the up-regulation of autophagy and with the transcrip-

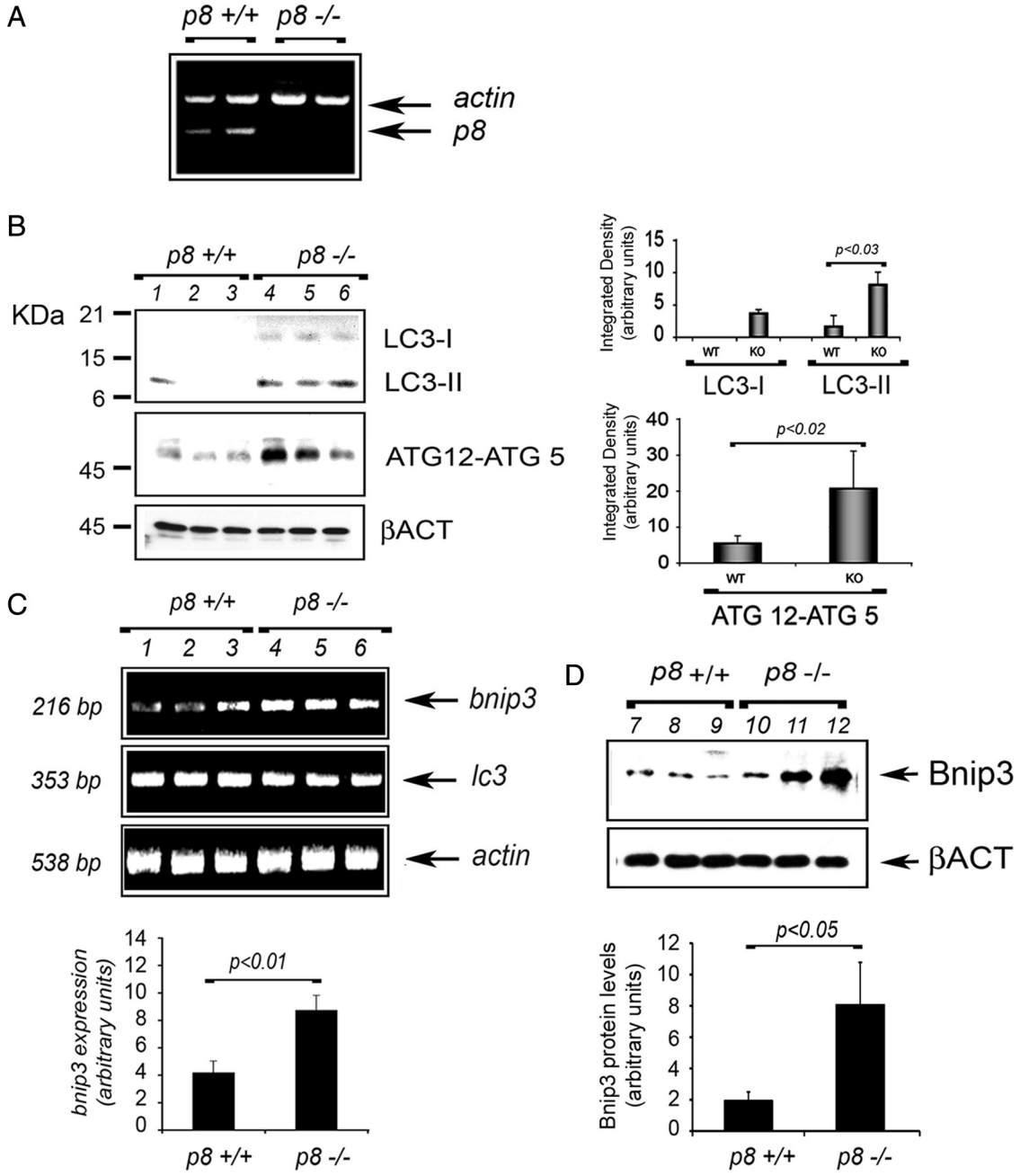

Figure 7. Cardiac tissue from *p8* −/− mice exhibits higher basal autophagy and present increased levels of both Bnip3 RNA and protein. (A) *p8* is expressed in the heart. RT-PCR analysis of total RNA from LVs of wilt type (*p8* +/+) and knockout mice (*p8* −/−). *p8* and *actin* were coamplified, and PCR products were separated on 1.8% agarose gel. (B) *p8* −/− mice have higher LC3-II and ATG12–5 levels. Western blot analysis of LV extracts from *p8* +/+ and *p8* −/− mice by using anti-LC3B, anti-ATG12-5, and β-actin antibodies. The quantifications are shown in the histograms. The values represent the mean ± SEM. Samples were subjected to unpaired Student's *t* test ($p < 0.03$ and $p < 0.02$, respectively; $n = 5$). (C) *p8* −/− mice have higher *bnip3* expression. *bnip3*, *lc3*, and *actin* were amplified from LV RNA of *p8* +/+ and *p8* −/− mice. PCR products were quantified and subjected to unpaired Student's *t* test ($p < 0.01$; $n = 6$). (D) *p8* −/−mice have higher Bnip3 protein levels. Western blot analysis of LV extracts from *p8* +/+ and *p8* −/− mice by using anti Bnip3 and β-actin antibodies, as indicated. The quantifications are shown in the histograms ($p < 0.05$; $n = 4$). The values represent the means ± SEM.

tion of a known FoxO3 target gene involved in the autophagic process.

Silencing of p8 Causes Autophagy and Apoptosis

Under basal conditions the low level of autophagy is tightly regulated and is required to maintain cellular homeostasis (Codogno and Meijer, 2005; Maiuri *et al*., 2007). The results we present show that basal *p8* expression represses autophagy and protects cells from autophagy-induced cell death. *p8* RNAi increases puncta formation, indicative of autophagosome accumulation, albeit to a lower level than rapamycin or serum starvation, two known inducers of autophagy. Autophagosomes accumulation can reflect either an increase of formation, due to an increase in autophagic activity, or a

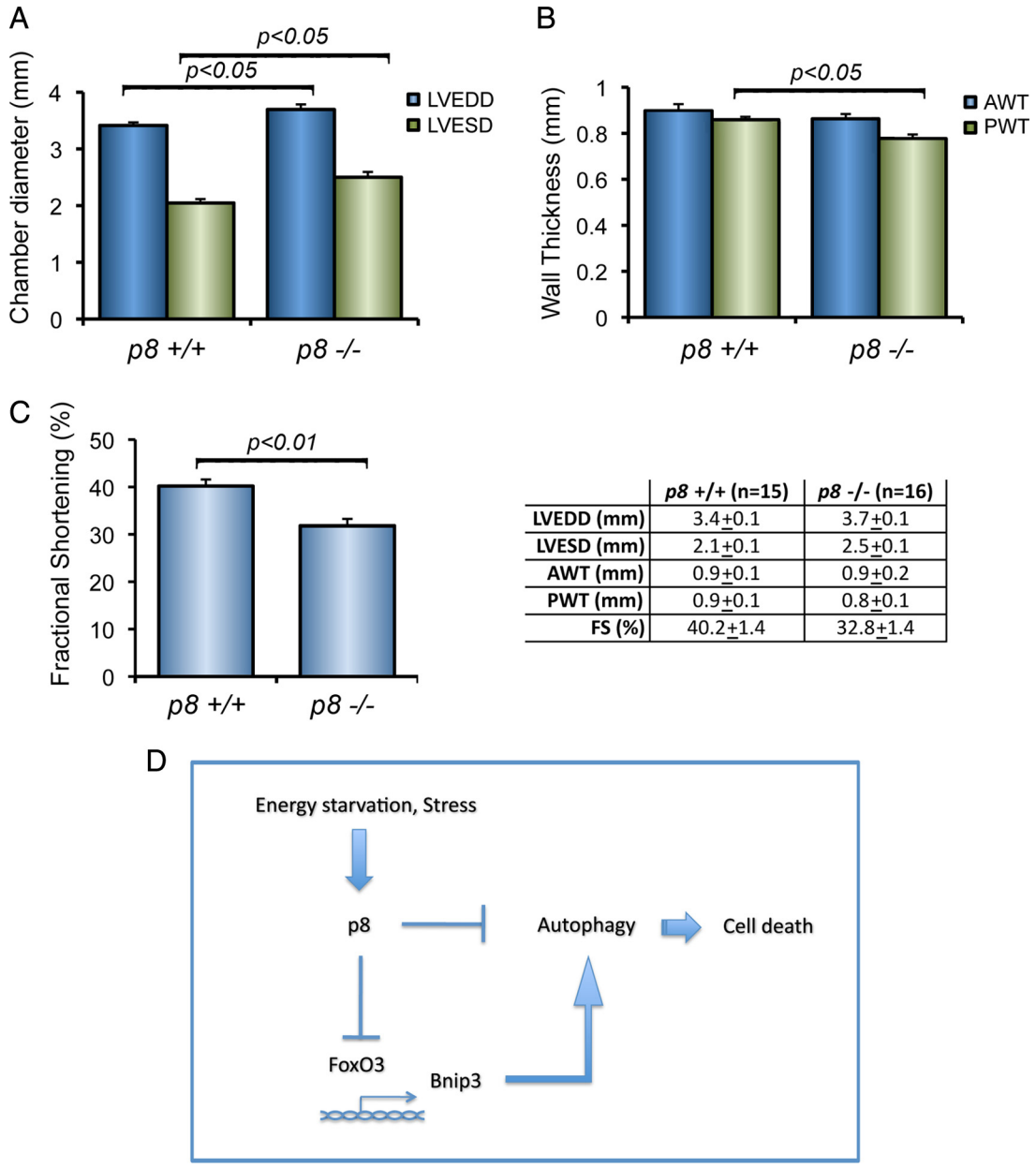

	p8 +/+ (n=15)	*p8* -/- (n=16)
LVEDD (mm)	3.4±0.1	3.7±0.1
LVESD (mm)	2.1±0.1	2.5±0.1
AWT (mm)	0.9±0.1	0.9±0.2
PWT (mm)	0.9±0.1	0.8±0.1
FS (%)	40.2±1.4	32.8±1.4

Figure 8. *p8* genetic deletion is associated with a cardiac phenotype. (A) *p8* −/− hearts display chamber dilation. Echocardiographic data from LV of *p8* +/+ and *p8* −/− mice (*p < 0.05); n = 15 for each group). LVEDD and LVESD are measured in millimeters. (B) *p8* −/− hearts display LV wall thinning. AWT and PW, anterior and posterior wall thickness (in millimeters) (*p < 0.05 for PWT +/+ vs. −/−; n = 15 for each group). (C) *p8* −/− mice have lower fractional shortening when compared with *p8* +/+ mice. FS, fractional shortening, calculated from A as (LVEDD − LVESD/LVEDD) × 100% (*p < 0.01 +/+ vs. −/−; n = 15). Numeric values for echocardiographic data are shown in the right panel. (D) Scheme of the mechanism regulating autophagy by p8.

reduction in their turnover. In our system, addition of autophagy inhibitors further increased both puncta formation and LC3 processing, strongly suggesting that *p8* silencing increases the on rate of the autophagic process. In addition, such LC3 processing was inhibited by *atg5* silencing, 3MA, and methyl pyruvate addition, pointing thus to a canonical autophagic pathway activation (Klionsky *et al.*, 2008).

Although enhanced autophagy may confer a growing advantage, a constant increase in self-cannibalism may reduce survival rates when environmental stresses appear. We show here that the inability to regulate *p8* renders the cells more sensitive to metabolic stressors. Accordingly, the mouse embryonic fibroblasts derived from p8 knockout mice have been shown to proliferate faster, but they fail to produce colonies when challenged in the absence of adhesion (Vasseur *et al.*, 2002a).

p8 Represses FoxO3 Transactivation of bnip3

p8 is activated by various stressors, including agents affecting DNA structure, cytokines, and growth conditions. This induction by stress involves multiple mechanisms that often lead to stabilization of the protein. Once activated, p8 mediates several effects ranging from genomic stability, apoptosis, cellular growth, and cell cycle arrest. Some of these

effects depend on p8 ability to modify transcriptional activity (Goruppi *et al*., 2007; Chowdhury *et al*., 2009). Whether p8 induces adaptive responses (cell survival) or cell death has been linked so far to distinct transcriptional programs and might depend on the stimuli or cellular microenvironment (Chowdhury *et al*., 2009; Goruppi and Iovanna, 2009). Our evidences indicate that p8 represses FoxO transcription and that *p8* absence is associated with increased FoxO3-dependent expression of *bnip3*, in vitro and in vivo.

FoxO3 controls the activation of autophagy, as overexpression of an activated FoxO3 induces autophagy in a muscle cell line and regulates the expression of *atgs* in the skeletal muscle (Mammucari *et al*., 2007; Zhao *et al*., 2007). In this setting, a key role is played by FoxO3-induced *bnip3*, because its overexpression stimulates autophagosome formation, whereas *bnip3* silencing decreases FoxO3-induced autophagy. Accordingly, we show that p8 represses Bnip3 up-regulation by AICAR that *bnip3* knockdown restores cell viability of *p8* deficient cells and blocks *p8* RNAi-induced apoptosis, thus reinforcing p8 corepressor role toward FoxO3. Nevertheless, *bnip3* RNAi does not completely restore cell viability of *p8* deficient cells, and these cells have yet higher autophagy levels, strongly pointing to the existence of additional proautophagic targets repressed by p8.

The precise mechanism of Bnip3 effects on autophagy remains to be determined. Bnip3 might induce autophagy (or apoptosis) by competing with Bcl2 and BclXL for Beclin1 interaction (Pattingre *et al*., 2005; Zhang and Ney, 2009). Accordingly, dissociation of Beclin1/BclXL complex by the BH3-mimetic peptide or after Dap-kinase phosphorylation promotes autophagy (Oltersdorf *et al*., 2005; Zalckvar *et al*., 2009). Alternatively, deregulated Bnip3 expression might cause mitochondrial damage, cytochrome *c* release, and reactive oxygen species increase (Zhang and Ney, 2009). Finally, Bnip3 has been shown also to inhibit mTOR, suggesting a path to cell death by protein synthesis inhibition (Li *et al*., 2007).

How Does p8 Regulate FoxO3 Activity?

FoxO localization is mostly determined by growth factors presence, and additional levels of regulation are represented by protein–protein interactions, acetylations, and phosphorylations (Arden, 2007; Calnan and Brunet, 2008). Some stressors, such as AMPK, can affect FoxO3 transcriptional activity without influencing its localization (Greer *et al*., 2007). p8 is primarily nuclear in subconfluent cells but can localizes throughout the cell in high density grown or in G0-arrested cells (Valacco *et al*., 2006). Our evidence show that *p8* silencing leads to an increase in basal nuclear FoxO3 and that p8 can be found in complex with FoxO3. It is possible that p8 interferes either with FoxO3 shuttling or with its interactions with other partners.

We have shown previously that p8 associates with *anf* and *mmp9* promoters in the cardiovascular system (Goruppi *et al*., 2007). Even though multiple FoxO consensus are present on *bnip3* promoter (Mammucari *et al*., 2007), our evidence do not point to a direct p8 competition with FoxO3 for the same DNA target, because p8 lacks transactivation activity toward the minimal consensus reporter. Finally, FoxO3 induces autophagy by stimulating the expression of several *atgs* and other genes; it is unlikely that Bnip3 represents the only FoxO3's target whose expression is repressed by p8. The effects on these additional autophagic genes remain to be determined.

Our research evidences a possible conundrum: p8 is transiently induced by autophagic stimuli while its presence represses the autophagy. Thus, p8 might represent an additional level of control toward FoxO3 functions, possibly acting as a feedback loop, which integrates signals sensing both growth factors and low AMP levels. Accordingly, AICAR and 2DG, but not serum deprivation, stabilize posttranslationally p8 polypeptide, and the effects of *p8* knockdown on cell viability are enhanced if cells are deprived of growth factors.

In the long-term, FoxO3-induced up-regulation of *atgs* has been proposed to be necessary to maintain active the autophagic machinery (Klionsky *et al*., 2008). Because prolonged autophagy by an energy stressor results in p8 down-regulation, p8 might participate in the integration of transient versus a more protracted cellular autophagy, acting as a transient feedback repressor for untimely FoxO3 transcription.

p8 Knockout Mice Develop a Decreased Left Ventricular Function

p8/Nupr1 is a stress-induced protein that is turned on by the cell's stress management program at times of emergencies (Chowdhury *et al*., 2009; Goruppi and Iovanna, 2009). Little is known regarding its basal functions in vivo. In the knockout mice, *p8* absence does not cause evident phenotypes, and animals were reported to develop normally (Vasseur *et al*., 2002b). Because we hypothesized previously a function for p8 in heart failure, our investigation was focused on the role of *p8* in the heart under basal conditions. We show here that *p8* silencing causes autophagy and apoptosis in cardiomyocytes and cardiac fibroblasts, two major heart cellular components, thus extending the relevance of our findings to the cardiovascular system.

Activation of autophagy plays a causative role in cardiomyopathy. Autophagic cell death as cause of cellular degeneration has been implicated in patients with hypertrophied and failing myocardium secondary to ischemia or dilated cardiomyopathy (De Meyer and Martinet, 2008). Incomplete autophagy in lysosome-associated protein 2-deficient mice provokes autophagosome accumulation and cardiomyopathy, whereas *atg5* deletion in the adult mice leads to hypertrophy and contractile disfunction (Nakai *et al*., 2007; De Meyer and Martinet, 2008). The general consensus indicates that at baseline autophagy represents a homeostatic mechanism for maintaining cardiomyocyte size and cellular structure (Rothermel and Hill, 2008b); further study will determine whether in *p8* mice changes in the cellular architecture or increased apoptosis are responsible for the functional phenotype.

The role of autophagy in the heart is still controversial. In an ischemia/reperfusion (I/R) model, the up-regulation of autophagy can protect from cell death, as either pharmacological inhibition or by interfering with *atg5* functions will worsen the consequences. Interestingly, much of the I/R damages seem mediated by Bnip3 up-regulation, as its overexpression causes myocytes autophagy and cell death, whereas its silencing rescues both (Hamacher-Brady *et al*., 2006; Hamacher-Brady *et al*., 2007). The inability to up-regulate autophagy during sustained pressure overload in mice with genetic disruption of *atg5* in the heart causes left ventricular dilation at a time when the wt animals develop compensatory hypertrophy (Nakai *et al*., 2007). Determining the effects of *p8* absence following heart pressure overload or in an animal swimming model will contribute to the understanding of the functions carried out by basal versus induced auto-

phagy in the heart and the role of FoxO3 transcription in this process. In addition, multiple pathophysiological conditions are associated with induction of autophagy. Fully understanding p8's multifaceted functions might open new avenues to the understanding of pathophysiological conditions associated with induction of autophagy, such as cardiovascular pathologies and cancer.

ACKNOWLEDGMENTS

We thank Marco Sandri (Padova University) and Alessia Di Nardo (Harvard University) for reagents and Joseph Alroy (Tufts University) for discussion and suggestions. C. C. was supported by "*la ligue contre le cancer.*" This work was supported by funds from American Heart Association grant SDG 0830359N (to S. G.) and National Institutes of Health grant R01-CA112399 (to J.M.K.).

REFERENCES

Arden, K. C. (2007). FoxOs in tumor suppression and stem cell maintenance. Cell *128*, 235–237.

Attaix, D., and Bechet, D. (2007). FoxO3 controls dangerous proteolytic liaisons. Cell Metab. *6*, 425–427.

Baehrecke, E. H. (2005). Autophagy: dual roles in life and death? Nat. Rev. Mol. Cell Biol. *6*, 505–510.

Brunet, A., Bonni, A., Zigmond, M. J., Lin, M. Z., Juo, P., Hu, L. S., Anderson, M. J., Arden, K. C., Blenis, J., and Greenberg, M. E. (1999). Akt promotes cell survival by phosphorylating and inhibiting a Forkhead transcription factor. Cell *96*, 857–868.

Calnan, D. R., and Brunet, A. (2008). The FoxO code. Oncogene *27*, 2276–2288.

Carracedo, A., *et al*. (2006). The stress-regulated protein p8 mediates cannabinoid-induced apoptosis of tumor cells. Cancer Cell *9*, 301–312.

Chowdhury, U. R., Samant, R. S., Fodstad, O., and Shevde, L. A. (2009). Emerging role of nuclear protein 1 (NUPR1) in cancer biology. Cancer Metastasis Rev. *28*, 225–232.

Clark, D. W., Mitra, A., Fillmore, R. A., Jiang, W. G., Samant, R. S., Fodstad, O., and Shevde, L. A. (2008). NUPR1 interacts with p53, transcriptionally regulates p21 and rescues breast epithelial cells from doxorubicin-induced genotoxic stress. Curr. Cancer Drug Targets *8*, 421–430.

Codogno, P., and Meijer, A. J. (2005). Autophagy and signaling: their role in cell survival and cell death. Cell Death Differ. *12* (suppl 2), 1509–1518.

De Meyer, G. R., and Martinet, W. (2008). Autophagy in the cardiovascular system. Biochim. Biophys. Acta *1793*, 1485–1495.

Furuyama, T., Nakazawa, T., Nakano, I., and Mori, N. (2000). Identification of the differential distribution patterns of mRNAs and consensus binding sequences for mouse DAF-16 homologues. Biochem. J. *349*, 629–634.

Goruppi, S., Bonventre, J. V., and Kyriakis, J. M. (2002). Signaling pathways and late-onset gene induction associated with renal mesangial cell hypertrophy. EMBO J. *21*, 5427–5436.

Goruppi, S., Chiaruttini, C., Ruaro, M. E., Varnum, B., and Schneider, C. (2001). Gas6 induces growth, beta-catenin stabilization, and T-cell factor transcriptional activation in contact-inhibited C57 mammary cells. Mol. Cell Biol. *21*, 902–915.

Goruppi, S., and Iovanna, J. L. (2009). The stress-inducible protein p8 is involved in several physiological and pathological processes. J. Biol. Chem. *285*, 1577–1581.

Goruppi, S., and Kyriakis, J. M. (2004). The pro-hypertrophic basic helix-loop-helix protein p8 is degraded by the ubiquitin/proteasome system in a protein kinase B/Akt- and glycogen synthase kinase-3-dependent manner, whereas endothelin induction of p8 mRNA and renal mesangial cell hypertrophy require NFAT4. J. Biol. Chem. *279*, 20950–20958.

Goruppi, S., Patten, R. D., Force, T., and Kyriakis, J. M. (2007). Helix-loop-helix protein p8, a transcriptional regulator required for cardiomyocyte hypertrophy and cardiac fibroblast matrix metalloprotease induction. Mol. Cell Biol. *27*, 993–1006.

Greer, E. L., Oskoui, P. R., Banko, M. R., Maniar, J. M., Gygi, M. P., Gygi, S. P., and Brunet, A. (2007). The energy sensor AMP-activated protein kinase directly regulates the mammalian FOXO3 transcription factor. J. Biol. Chem. *282*, 30107–30119.

Hamacher-Brady, A., Brady, N. R., Gottlieb, R. A., and Gustafsson, A. B. (2006). Autophagy as a protective response to Bnip3-mediated apoptotic signaling in the heart. Autophagy *2*, 307–309.

Hamacher-Brady, A., Brady, N. R., Logue, S. E., Sayen, M. R., Jinno, M., Kirshenbaum, L. A., Gottlieb, R. A., and Gustafsson, A. B. (2007). Response to myocardial ischemia/reperfusion injury involves Bnip3 and autophagy. Cell Death Differ. *14*, 146–157.

Hardie, D. G. (2007). AMP-activated/SNF1 protein kinases: conserved guardians of cellular energy. Nat. Rev. Mol. Cell Biol. *8*, 774–785.

Herrero-Martin, G., Hoyer-Hansen, M., Garcia-Garcia, C., Fumarola, C., Farkas, T., Lopez-Rivas, A., and Jaattela, M. (2009). TAK1 activates AMPK-dependent cytoprotective autophagy in TRAIL-treated epithelial cells. EMBO J. *28*, 677–685.

Hoffmeister, A., *et al*. (2002). The HMG-I/Y-related protein p8 binds to p300 and Pax2 trans-activation domain-interacting protein to regulate the trans-activation activity of the Pax2A and Pax2B transcription factors on the glucagon gene promoter. J. Biol. Chem. *277*, 22314–22319.

Klionsky, D. J., *et al*. (2008). Guidelines for the use and interpretation of assays for monitoring autophagy in higher eukaryotes. Autophagy *4*, 151–175.

Kundu, M., and Thompson, C. B. (2008). Autophagy: basic principles and relevance to disease. Annu. Rev. Pathol. *3*, 427–455.

Levine, B., and Kroemer, G. (2008). Autophagy in the pathogenesis of disease. Cell *132*, 27–42.

Li, Y., Wang, Y., Kim, E., Beemiller, P., Wang, C. Y., Swanson, J., You, M., and Guan, K. L. (2007). Bnip3 mediates the hypoxia-induced inhibition on mammalian target of rapamycin by interacting with Rheb. J. Biol. Chem. *282*, 35803–35813.

Maiuri, M. C., Zalckvar, E., Kimchi, A., and Kroemer, G. (2007). Self-eating and self-killing: crosstalk between autophagy and apoptosis. Nat. Rev. Mol. Cell Biol. *8*, 741–752.

Malicet, C., Dagorn, J. C., Neira, J. L., and Iovanna, J. L. (2006). p8 and prothymosin alpha: unity is strength. Cell Cycle *5*, 829–830.

Mammucari, C., *et al*. (2007). FoxO3 controls autophagy in skeletal muscle in vivo. Cell Metab. *6*, 458–471.

Meijer, A. J., and Codogno, P. (2008). Nutrient sensing: TOR's Ragtime. Nat. Cell Biol. *10*, 881–883.

Mizushima, N., Levine, B., Cuervo, A. M., and Klionsky, D. J. (2008). Autophagy fights disease through cellular self-digestion. Nature *451*, 1069–1075.

Nakai, A., *et al*. (2007). The role of autophagy in cardiomyocytes in the basal state and in response to hemodynamic stress. Nat. Med. *13*, 619–624.

Oltersdorf, T., *et al*. (2005). An inhibitor of Bcl-2 family proteins induces regression of solid tumours. Nature *435*, 677–681.

Pattingre, S., Tassa, A., Qu, X., Garuti, R., Liang, X. H., Mizushima, N., Packer, M., Schneider, M. D., and Levine, B. (2005). Bcl-2 antiapoptotic proteins inhibit Beclin 1-dependent autophagy. Cell *122*, 927–939.

Polager, S., Ofir, M., and Ginsberg, D. (2008). E2F1 regulates autophagy and the transcription of autophagy genes. Oncogene *27*, 4860–4864.

Quirk, C. C., Seachrist, D. D., and Nilson, J. H. (2003). Embryonic expression of the luteinizing hormone beta gene appears to be coupled to the transient appearance of p8, a high mobility group-related transcription factor. J. Biol. Chem. *278*, 1680–1685.

Rothermel, B. A., and Hill, J. A. (2008a). Autophagy in load-induced heart disease. Circ. Res. *103*, 1363–1369.

Rothermel, B. A., and Hill, J. A. (2008b). The heart of autophagy: deconstructing cardiac proteotoxicity. Autophagy *4*, 932–935.

Salazar, M., *et al*. (2009). Cannabinoid action induces autophagy-mediated cell death through stimulation of ER stress in human glioma cells. J. Clin. Invest. *119*, 1359–1372.

Sambasivan, R., Cheedipudi, S., Pasupuleti, N., Saleh, A., Pavlath, G. K., and Dhawan, J. (2009). The small chromatin-binding protein p8 coordinates the association of anti-proliferative and pro-myogenic proteins at the myogenin promoter. J. Cell Sci. *122*, 3481–3491.

Valacco, M. P., Varone, C., Malicet, C., Canepa, E., Iovanna, J. L., and Moreno, S. (2006). Cell growth-dependent subcellular localization of p8. J. Cell Biochem. *97*, 1066–1079.

Vasseur, S., Hoffmeister, A., Garcia, S., Bagnis, C., Dagorn, J. C., and Iovanna, J. L. (2002a). p8 is critical for tumour development induced by rasV12 mutated protein and E1A oncogene. EMBO Rep. *3*, 165–170.

Vasseur, S., Hoffmeister, A., Garcia-Montero, A., Mallo, G. V., Feil, R., Kuhbandner, S., Dagorn, J. C., and Iovanna, J. L. (2002b). p8-deficient fibroblasts grow more rapidly and are more resistant to Adriamycin-induced apoptosis. Oncogene *21*, 1685–1694.

Xie, Z., and Klionsky, D. J. (2007). Autophagosome formation: core machinery and adaptations. Nat. Cell Biol. *9*, 1102–1109.

Zalckvar, E., Berissi, H., Mizrachy, L., Idelchuk, Y., Koren, I., Eisenstein, M., Sabanay, H., Pinkas-Kramarski, R., and Kimchi, A. (2009). DAP-kinase-mediated phosphorylation on the BH3 domain of beclin 1 promotes dissociation of beclin 1 from Bcl-XL and induction of autophagy. EMBO Rep. *10*, 285–292.

Zhang, J., and Ney, P. A. (2009). Role of BNIP3 and NIX in cell death, autophagy, and mitophagy. Cell Death Differ. *16*, 939–946.

Zhao, J., Brault, J. J., Schild, A., Cao, P., Sandri, M., Schiaffino, S., Lecker, S. H., and Goldberg, A. L. (2007). FoxO3 coordinately activates protein degradation by the autophagic/lysosomal and proteasomal pathways in atrophying muscle cells. Cell Metab. *6*, 472–483.